# Whispering-gallery-mode terahertz pulse propagation on a curved metallic plate

Rajind Mendis[a] and Daniel M. Mittleman
*Department of Electrical and Computer Engineering, MS-366, 6100 Main Street, Rice University, Houston, Texas 77005, USA*

(Received 17 June 2010; accepted 28 June 2010; published online 19 July 2010)

We demonstrate terahertz (THz) pulse propagation on a cylindrical aluminum plate, with low loss and negligible dispersion via transverse-electric type whispering gallery (WG) modes. We observe an apparent superluminal effect where the group velocity is greater than $c$, and explain this phenomenon by means of a plane-wave description of the WG modes. The propagation loss is dominated by the diffraction loss due to unbounded lateral spreading, with a negligible ohmic-loss contribution. Both experimental and theoretical results indicate a total loss as low as 2.6 dB/m at a frequency of 0.47 THz. © *2010 American Institute of Physics*. [doi:10.1063/1.3466909]

It is well known that electromagnetic-wave modes in a parallel-plate waveguide (PPWG) (Ref. 1) can be analyzed in terms of traveling plane waves, continuously reflecting back and forth between the two metallic plates.[2] Assuming this bouncing plane-wave picture holds even when the PPWG is curved, a natural consequence would be the possibility of guiding energy using only a single curved (concave) plate, provided there is sufficient curvature to sustain continuous reflections. This waveguiding concept is analogous to the "whispering gallery" (WG) modes first demonstrated by Rayleigh,[3] in which acoustic waves were found to cling to and follow a concave surface. Generally, there can be two manifestations of these WG modes: one where the wave undergoes *total reflection* at a curved metallic surface,[4,5] and the other where the wave undergoes *total internal reflection* at a curved boundary between two dielectric media.[6–8] Here, we demonstrate the former in the terahertz (THz) frequency regime, and determine the loss and dispersion characteristics of this curved waveguide.

For the experiment, we use a system that generates picosecond THz pulses having a fiber-coupled transmitter and receiver. We start with the waveguide configuration shown in the left inset of Fig. 1, fabricated using polished aluminum plates. This composite PPWG has a 3 cm straight section followed by a semicircular section having radii of 7 and 8 cm for the inner and outer plates. The fabrication was such that the curved inner plate could be detached leaving the 25.1 cm long curved outer plate and the straight PPWG section intact, as shown in the right inset. The THz beam was coupled in through the straight PPWG section, polarized parallel to the plates, to excite the $TE_1$ mode in this section.[2] The blue trace in Fig. 1 shows the THz signal that has propagated through the composite PPWG. This signal exhibits good single-mode behavior with low loss and negligible dispersion. When the inner plate is detached (right inset), we observe the signal shown by the red trace in Fig. 1. Remarkably, the main THz pulse is almost indistinguishable from that of the previous configuration. This indicates that the inner curved plate has minimal affect on the propagating signal, implying that energy is mostly concentrated near the outer plate in the curved section. To investigate this further, we formed a variable slit near the surface of the plate using a flat aluminum plate, at three different positions [input, center (as shown in the inset), and output] along the curved path, and measured the propagated signal. Figure 2 plots the peak positive amplitude of the main pulse of this signal as a function of the slit opening $d$. This confirms that energy is well confined within 1 cm from the plate surface, while being guided along the curved path.

Following the theoretical analysis in Ref. 9, which involves a conformal mapping from cylindrical to rectangular coordinates under the assumption that the radius-of-curvature $R \gg \lambda$, we calculate the propagation constants for the TE-type WG modes. These are then used to derive the frequency dependent phase ($v_p$) and group ($v_g$) velocities for the three lowest-order TE-type WG modes for our case of $R=8$ cm. These results are plotted in Fig. 3, along with the experimental values (dots) derived by comparing the phase of the propagated pulse of the WG waveguide (right inset of Fig. 1) to that of the output of a 3 cm long straight PPWG identical to the one in the original composite. The agreement between experiment and theory (for the $WG_1$ mode) is reasonably good, and is seen to improve as $\lambda$ decreases, consis-

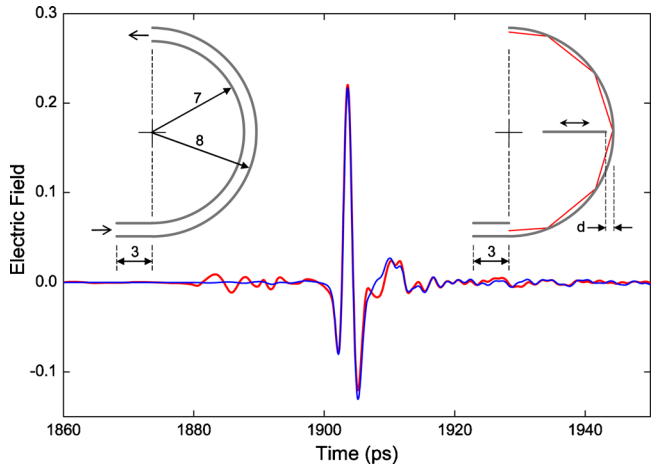


FIG. 1. (Color online) The blue trace is the THz waveform corresponding to the composite PPWG in the left inset, while the red trace is the one when the inner plate is detached as in the right inset. The right inset shows a flat aluminum plate forming a slit at the center, and also the polygonal chain (red) depicting the plane-wave path of the WG mode.

[a]Electronic mail: rajind@rice.edu.

 

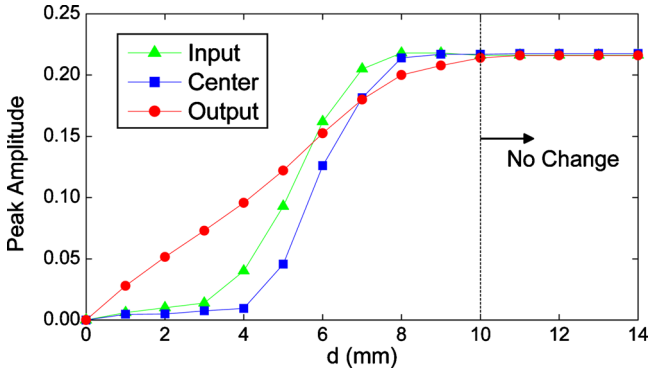


FIG. 2. (Color online) The peak positive amplitude of the propagated signal as a function of the slit opening $d$, formed at the input, center, and output of the curved plate. There is no change in signal after 10 mm.

tent with the primary theoretical assumption that $R \gg \lambda$.

This analysis reveals several important points. First, we note that WG modes do not have low-frequency cutoffs, which is consistent with the single boundary of the guiding structure. Second, we note an extraordinary superluminal effect, where $v_g > c$, which is rarely observed in practical waveguides. At the same time, since $v_p > v_g$, this represents a regime of *normal dispersion*, and it is safe to say that $v_g$ represents the velocity of energy propagation.[10] However, this poses a quandary since energy cannot obviously propagate faster than $c$. We resolve this by resorting to the plane-wave description of WG modes as illustrated by the red *polygonal chain* shown in the right inset of Fig. 1. This shows that the path-length traveled by this equivalent plane wave is shorter than the circumferential path-length traveled by an idealized reference wave. This geometric effect mathematically results in $v_g > c$ for the WG modes considered here, but does not amount to superluminal energy propagation. We have also plotted the mode profiles of the three lowest-order WG modes in Fig. 4, which indicate that energy becomes less concentrated to the plate as the mode number increases. For a given mode this occurs when the frequency decreases. This is consistent with the increase in velocity as the mode number increases, and also when the frequency decreases for a given mode, as seen in Fig. 3.

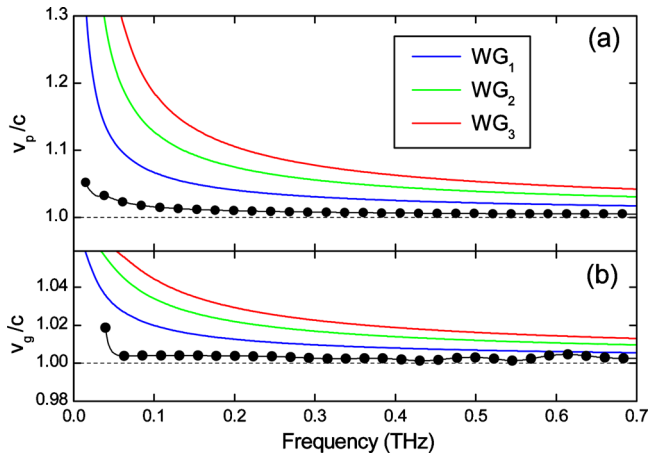


FIG. 3. (Color online) The frequency dependence of the phase (a), and group (b) velocity of the three lowest-order TE-type WG modes based on theory, compared to the experimental values (dots).

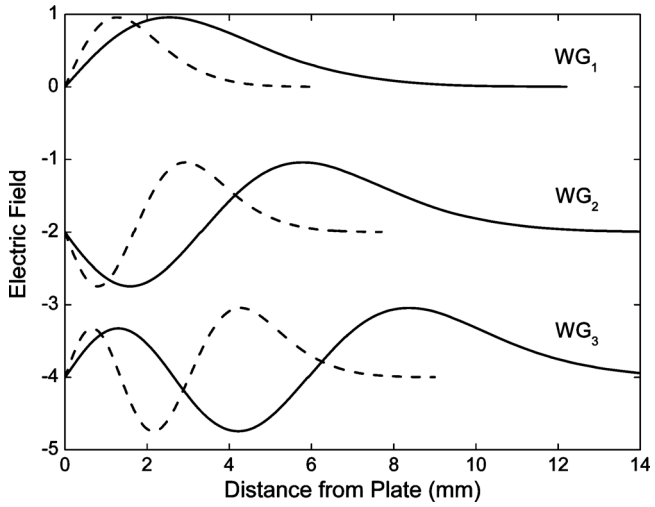


FIG. 4. The spatial electric field profiles of the three lowest-order TE-type WG modes at 0.1 THz (solid curves) and 0.3 THz (dashed curves) based on theory. The profiles are vertically offset for clarity.

The ohmic (resistive) loss introduced by the curved metallic plate can be theoretically analyzed using the bouncing plane-wave description of the WG modes, similar to previous work on PPWGs.[2] Here, the loss per unit (curved) length is derived as

$$\alpha_R = N(1 - |r_s|^2), \tag{1}$$

where $r_s$ is the reflection coefficient at the air-metal boundary for $s$-polarized incidence and $N$ is the number of bounces per unit length. We can show that $N = 1/[R(\pi - 2\theta)]$, where $\theta$ is the angle of incidence at each bounce [inset of Fig. 5(a)]. To be consistent with the velocity curves, the total path-length of the plane wave supported by a given curved plate, has to decrease as the frequency decreases, resulting in a decreasing $\theta$ as well as a decreasing $N$. By equating the relevant component of the propagation constant derived using the previous theoretical analysis[9] to that of the bouncing plane wave, we obtain the frequency dependence of $\theta$. This is plotted in Fig. 5(a), along with that of $N$, for the $WG_1$ mode. These curves show that both $\theta$ and $N$ increase with increasing frequency, as expected. It is interesting to note that the frequency dependence of $N$ is in direct contrast to that observed for the $TE_1$ mode of the PPWG. For the $TE_1$ mode, $N$ decreases with increasing frequency, which was influential in bringing down $\alpha_R$ as the frequency increases.[2] Therefore, here we expect the opposite frequency dependence in $\alpha_R$ for the $WG_1$ mode. Since $N$ is known, and $r_s$ can be calculated for the air-aluminum boundary, we can derive $\alpha_R$ using Eq. (1). This is plotted in Fig. 5(b), along with that for the $TE_1$ mode of a PPWG (plate-separation=1 cm). The ohmic loss is $2.2 \times 10^{-4}$ dB/cm for both modes at 0.06 THz (cross-over point), and $6.4 \times 10^{-4}$ dB/cm for the $WG_1$ mode and $9.3 \times 10^{-6}$ dB/cm for the $TE_1$ mode at 0.5 THz. In practice, there will be an additional *diffraction loss* that manifests as a reduced energy coupling to the receiver (with a finite input aperture) due to unbounded diffractive spreading.[2,11]

To estimate the experimental propagation losses, we follow the analysis in Ref. 11 and apply the generalized input-output expression separately to the WG waveguide and a 3 cm long PPWG, to obtain

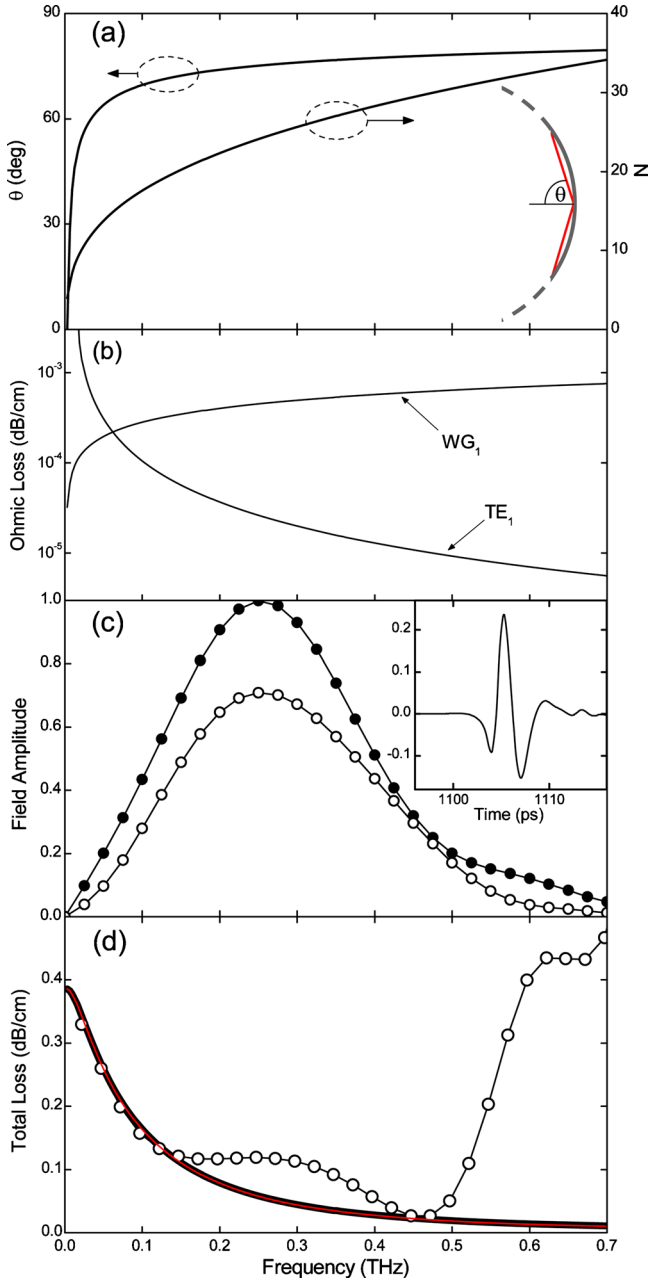


FIG. 5. (Color online) (a) Frequency dependence of the incidence angle $\theta$ (left vertical axis) and the number of bounces $N$ (right vertical axis), for the plane wave corresponding to the $WG_1$ mode as depicted in the inset. (b) Comparison of the ohmic loss $\alpha_R$ for the $WG_1$ mode and the $TE_1$ mode of a PPWG. (c) Amplitude spectra corresponding to the outputs of the WG waveguide (open circles) and a 3 cm long PPWG (dots). The output of the 3 cm PPWG is shown inset. (d) Experimental (open circles) and theoretical (solid black curve) comparison of the total loss $\alpha_T$. The red solid curve, almost perfectly overlapping with the black curve, gives the theoretical diffraction loss $\alpha_D$.

$$\left|\frac{E_{o2}}{E_{o1}}\right| = \frac{C_2}{C_1} e^{-\alpha_R(L_2-L_1)} = e^{-\alpha_T(L_2-L_1)}, \tag{2}$$

where the subscripts "1" and "2" stand for the two waveguides. $E_o$ is the output electric field, $C$ is the output coupling coefficient parallel to the plate surface, and $L$ is the propagation length. $C$ accounts for the diffractive spreading, and is calculated using the standard overlap-integral method.[12] Here, $\alpha_T$ is artificially defined to give the total loss accounting for both the diffraction loss and the ohmic loss. Rearranging Eq. (2), we can derive an expression for $\alpha_T$ as

$$\alpha_T = \alpha_R + \frac{1}{(L_1 - L_2)} \ln\left[\frac{C_2}{C_1}\right] = \alpha_R + \alpha_D, \tag{3}$$

where $\alpha_D = [1/(L_1 - L_2)]\ln[C_2/C_1]$ accounts for the diffraction loss and $L_2 - L_1 = 25.1$ cm. Figure 5(c) gives typical amplitude spectra corresponding to the truncated output pulse of the WG waveguide and that of the 3 cm PPWG (inset). Applying Eq. (2) to these spectra, we can derive the experimental $\alpha_T$, which is shown by the connected open circles in Fig. 5(d). The thick solid black curve gives the theoretical $\alpha_T$ obtained using Eqs. (1) and (3). The solid red curve, which is almost perfectly overlapping with the black curve, gives $\alpha_D$ alone, and indicates that the ohmic loss is negligible compared to the diffraction loss. Also, as expected, $\alpha_D$ increases with decreasing frequency, since the low frequencies diverge more strongly with propagation. A possible method to mitigate this diffraction loss would be to provide a slight curvature to the metallic plate in the transverse direction,[2] effectively forming a *biconcave* plate.

The experimental and theoretical $\alpha_T$ in Fig. 5(d) show good agreement toward the low-frequency end, while they tend to deviate toward the high-frequency end. This discrepancy could result from several factors. First, we considered the output of the 3 cm PPWG to be the input to the curved plate in the data analysis of the WG waveguide. Clearly, there will be some mode *mismatch* when energy couples from the PPWG-section to the curved plate. This mismatch becomes more severe as the frequency increases due to the frequency dependence in the $WG_1$ mode profile (Fig. 4). In addition, other loss mechanisms such as surface roughness become more significant at higher frequencies. Nevertheless, our experimental and theoretical results indicate that $\alpha_T$ can be as low as 2.6 dB/m at 0.47 THz.

In conclusion, we have introduced a family of THz waveguides that utilize curved metallic surfaces, where energy propagates via WG modes. This concept can be easily extended to design high-$Q$ resonant cavities for the THz regime. This concept can also be applied to incorporate sharp bends into PPWGs, compared to traditional miter bends[13] that could result in pulse distortion due to mode mixing. Incidentally, we note that these WG modes cannot exist on *flat* metallic surfaces and are thus distinct from Zenneck surface waves.[14]

This work was supported in part by the National Science Foundation and by the Air Force Research Laboratory through the CONTACT program.

[1] R. Mendis and D. Grischkowsky, Opt. Lett. **26**, 846 (2001).
[2] R. Mendis and D. M. Mittleman, J. Opt. Soc. Am. B **26**, A6 (2009).
[3] L. Rayleigh, Philos. Mag. **20**, 1001 (1910).
[4] E. Garmire, T. McMahon, and M. Bass, Appl. Phys. Lett. **31**, 92 (1977).
[5] J. Jiao and M. E. Marhic, Appl. Opt. **29**, 2793 (1990).
[6] J. R. Wait, Electron. Lett. **4**, 377 (1968).
[7] S. Sheem and J. R. Whinnery, Wave Electron. **1**, 61 (1974).
[8] J. Zhang and D. Grischkowsky, J. Opt. Soc. Am. B **20**, 1894 (2003).
[9] H. Krammer, Appl. Opt. **17**, 316 (1978).
[10] E. Hecht, *Optics* (Addison-Wesley, San Francisco, 2002).
[11] R. Mendis and D. M. Mittleman, Opt. Express **17**, 14839 (2009).
[12] R. Mendis and D. Grischkowsky, IEEE Microw. Wirel. Compon. Lett. **11**, 444 (2001).
[13] J. J. Campbell and W. R. Jones, IEEE Trans. Microwave Theory Tech. **16**, 517 (1968).
[14] T.-I. Jeon and D. Grischkowsky, Appl. Phys. Lett. **88**, 061113 (2006).